Electronic structure of the organic semiconductor Alq_3 (aluminum tris-8-hydroxyquinoline) from soft x-ray spectroscopies and density functional theory calculations

A. DeMasi,[1] L. F. J. Piper,[1] Y. Zhang,[1,a)] I. Reid,[1,b)] S. Wang,[1,c)] K. E. Smith,[1,d)] J. E. Downes,[2] N. Peltekis,[3] C. McGuinness,[3] and A. Matsuura[4]
[1]*Department of Physics, Boston University, Boston, Massachussets 02215, USA*
[2]*Department of Physics, Division of ICS, Macquarie University, New South Wales 2109, Australia*
[3]*School of Physics, Trinity College Dublin, University of Dublin, Dublin 2, Ireland*
[4]*In-Q-Tel, Arlington, Virginia 22203, USA*

(Received 5 August 2008; accepted 28 October 2008; published online 10 December 2008)

The element-specific electronic structure of the organic semiconductor aluminum tris-8-hydroxyquinoline (Alq_3) has been studied using a combination of resonant x-ray emission spectroscopy, x-ray photoelectron spectroscopy, x-ray absorption spectroscopy, and density functional theory (DFT) calculations. Resonant and nonresonant x-ray emission spectroscopy were used to measure directly the carbon, nitrogen and oxygen 2*p partial* densities of states in Alq_3, and good agreement was found with the results of DFT calculations. Furthermore, resonant x-ray emission at the carbon *K*-edge is shown to be able to measure the partial density of states associated with individual C sites. Finally, comparison of previous x-ray emission studies and the present data reveal the presence of clear photon-induced damage in the former. © *2008 American Institute of Physics*. [DOI: 10.1063/1.3030975]

I. INTRODUCTION

Organic electronic materials have been the subject of intense study for many years due to the potential advantages of carbon-based electronic devices over traditional inorganic semiconductor devices. Of particular interest are thin film materials that can be used in organic light emitting diodes (OLEDs).[1] Aluminum tris-(8-hydroxyquinolate) (Alq_3) is one of the key electroluminescent materials used today in such OLED devices.[2] Despite this, there have been few comprehensive studies of the electronic structure of Alq_3 using synchrotron radiation-based soft x-ray techniques. Accurate experimental determination of the electronic structure of thin film organic semiconductors is a prerequisite in developing a comprehensive understanding of such materials.

We report here an extensive experimental and theoretical investigation of the electronic structure of thin films of Alq_3 using synchrotron radiation-excited soft x-ray emission spectroscopy (XES), soft x-ray absorption spectroscopy (XAS), and photoelectron spectroscopy, together with density functional theory (DFT) calculations. Of particular note is the use of resonant soft XES (RXES). RXES is a powerful spectroscopic probe that can provide bulk sensitive and chemical site-specific electronic structure information.[3] RXES has already proven its ability to provide detailed information regarding the states near the Fermi level (E_F) for a range of organic compounds, including the metal phthalocyanines (Pc), such as Cu-Pc,[4] Sn-Pc,[5] VO-PC,[6,7] and TiO-Pc.[8] Our C, N, and O *K*-edge soft x-ray emission spectra from Alq_3 are in excellent agreement with the corresponding DFT calculated partial densities of states (PDOSs), but differ from a previous x-ray emission study.[9] We show that the difference is likely due to photon-induced beam damage of the samples in the earlier study.[9] X-ray photoemission spectroscopy (XPS) and XAS have also been used previously to investigate the occupied and unoccupied states of Alq_3 with comparison to DFT calculations of the density of states (DOS).[10,11] Our valence band XPS (VB-XPS) of thin Alq_3 films was found to be in agreement with earlier studies by Curioni *et al.*[10]

II. EXPERIMENT

Thin films of Alq_3 were grown *in situ* in a custom designed ultrahigh vacuum organic molecular beam deposition (OMBD) chamber (base pressure 2×10^{-9} torr), attached to a multitechnique soft x-ray spectroscopy system, described below. The substrates were *p*-type Si (100) wafers, ultrasonically cleaned in acetone before introduction into the OMBD system. Once in vacuum, the substrates were heated to 800 °C for 2 min. Alq_3 was deposited onto the substrate from a well outgassed glass crucible, which was heated by passing current through an encircling tantalum coil. The substrate was at room temperature during deposition. The deposition rate, monitored by a quartz crystal microbalance, was 0.01 nm/s. We found that a film of roughly 30 ML (monolayer) was thick enough to suppress photoemission from the

a)Present address: Department of Chemistry, University of Nevada Las Vegas, Las Vegas, NV 89154.
b)Present address: School of Physical Sciences, Dublin City University, Dublin, Ireland.
c)Present address: Department of Physics, Renmin University of China, China.
d)Author to whom correspondence should be addressed. Electronic mail: ksmith@bu.edu.

Si substrate, but was also sufficiently thin that no charging effects were apparent during XPS studies. The low intensity signal associated with RXES experiments requires a thicker sample. Consequently, the thickness of deposited films used in RXES was approximately 100 nm. XAS measurements of films of either thickness were found to be identical. After deposition, the samples were immediately transferred under vacuum into the spectrometer chamber (base pressure of 2×10^{-10} torr).

Experiments were performed at the soft x-ray undulator beamline X1B at the National Synchrotron Light Source (NSLS), Brookhaven National Laboratory, which is equipped with a spherical grating monochromator. The photon beam is focused to an approximate $60\times40\,\mu m^2$ spot on the sample. X-ray emission spectra were recorded with a Nordgren-type grazing incidence grating spectrometer.[12] XES involves the measurement of the photon emitted when a valence electron makes a radiative transition into a hole on a localized core level created by excitation of a core electron. In general, the resultant spectrum reflects the VB DOS. Furthermore, since strong dipole selection rules govern the transition, XES directly measures the orbital angular momentum resolved DOS, i.e., the PDOS.[13,14] Additional information can be extracted from emission spectra if the incident monochromatic synchrotron radiation is tuned to an energy close to a core absorption threshold. This variant is referred to as RXES. In this resonant case, the excited electron resides in a conduction band or lowest unoccupied molecular orbital (LUMO) state, and the system does not become ionized. If the system exhibits core level binding energy shifts due to different chemical bondings or site symmetries, holes can be resonantly created on each core level in turn as the excitation energy is increased, and thus the PDOS associated with a particular bond or chemical environment can be measured.[13]

The energy resolution for XES spectra presented here was approximately 0.4 eV near the carbon *K*-edge, and 0.6 eV near the nitrogen and oxygen *K*-edges. The energy scale of the C *K*-edge emission spectra was calibrated with third order Ni L_α/L_β metal emission, while the N *K*-edge emission spectra were calibrated with second order Co L_α/L_β emission, and the O *K*-edge spectra with second order Zn L_α/L_β.[15] XAS spectra were recorded by the sample drain current technique to obtain the total electron yield, and were normalized to the current from a Au coated mesh, placed in the path of the incident beam. The energy scale of the XAS measurements was calibrated using known absorption features of rutile TiO_2.[16] The calibration methods for XES and XAS are consistent with each other, and confirmed by the agreement between the XES elastic emission features and the positions of chosen excitation energies on the XAS spectra. The energy resolution for XAS is approximately 0.2 eV at the carbon and nitrogen *K*-edges, and 0.3 eV at the oxygen *K*-edge. Core level XPS spectra were recorded using a Scienta 100 mm hemispherical electron analyzer, with a 0.6 eV total energy resolution for the C 1*s*, N 1*s*, and O 1*s* levels. Binding energies are referenced relative to the binding energy of the Au $4f_{7/2}$ core level set at 84.0 eV, as measured from a gold foil in electrical contact with the sample, with the spectra presented relative to the Fermi energy of the Au foil, which is set to zero. The total instrumental resolution of the VB-XPS, calculated from the gold Fermi edge, was determined to be approximately 0.35 eV for $h\nu=250$ eV.

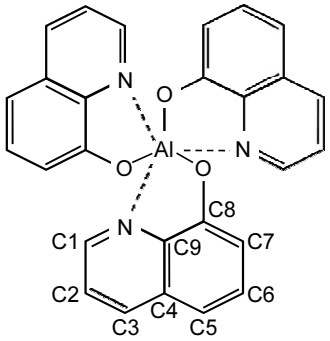

FIG. 1. Schematic representation of the Alq_3 molecule.

III. THEORETICAL DETAILS

The Alq_3 molecule consists of an aluminum atom bonded to three identical hydroxyquinoline ligands (Fig. 1). Alq_3 can exist as either of two isomers, dubbed facial and meridianal, which have C_3 and C_1 symmetries, respectively.[17] The meridianal isomer is the more energetically favorable form, and it will be especially dominant in films produced by evaporation onto a substrate, such as those in this study.[10,17] Consequently, all theoretical results discussed here are for the meridianal form of Alq_3. The DFT calculations used the generalized gradient approximation, B88:PW91 exchange-correlation functional, and a spin-restricted model. Parallel DGAUSS under *ab initio* CAChe (Fujitsu) was used to perform the calculation.

The three hydroxyquinoline ligands, being of identical structure and similar orientation, necessarily have comparable electronic structures; their densities of states are shifted relative to one another due to the lowered symmetry of the meridianal isomer resulting in triplet states, although the shifts are smaller than can be properly resolved by our techniques. This is shown in the calculated total DOS for each ligand in Fig. 2(a), which displays a 0.3 eV difference spanning the energy separation of equivalent features between the three ligands (e.g., the LUMO on ligand B and the LUMO″ on ligand A). Direct transitions are unlikely to occur between the actual HOMO and LUMO because they are on different ligands, as shown by Figs. 2(b) and 2(c). We instead characterize the electronic states not in terms of the entire molecule but rather in terms of an individual ligand. For instance, if we consider a transition from the highest occupied molecular orbital (HOMO) in Fig. 2(b) to the LUMO″ in Fig. 2(d) on ligand A, we may reasonably view this instead as a HOMO-LUMO transition, with the understanding that each state actually exists as a triplet.

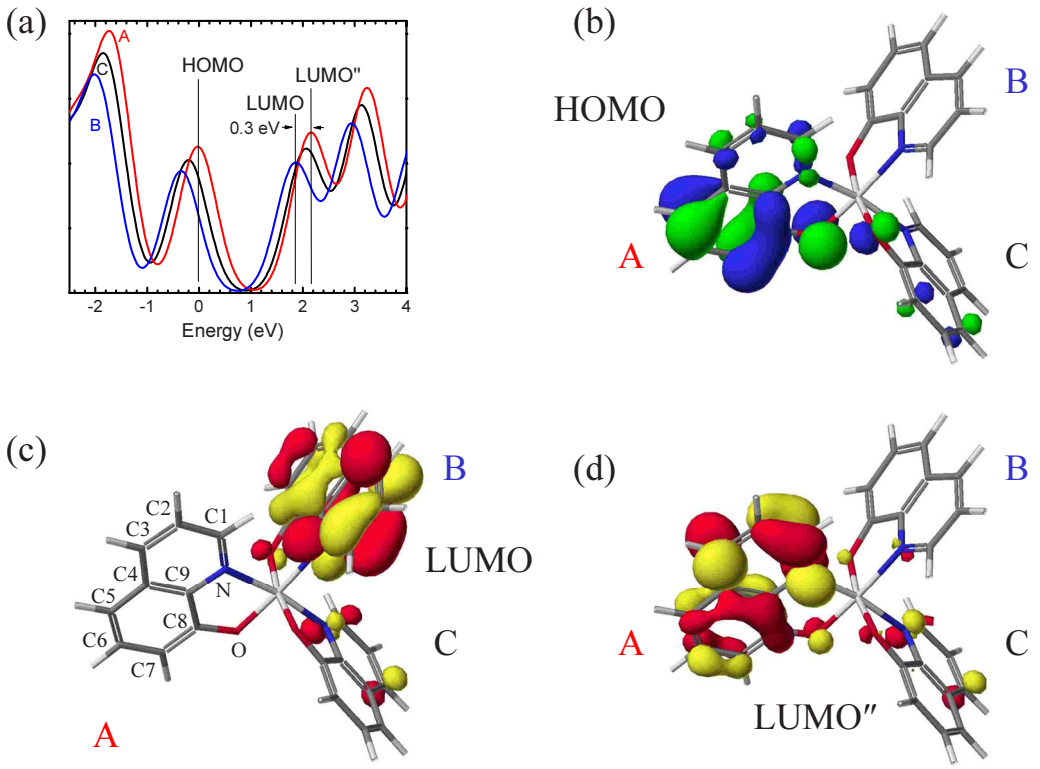

FIG. 2. (Color online) (a) DFT calculated total DOS near E_F for the three ligands: A, B, and C. The isodensity distribution of the (b) HOMO, (c) LUMO, and (d) LUMO+2 states in the meridianal isomer.

IV. RESULTS AND DISCUSSION

A. Photoemission spectroscopy

XPS ($h\nu$=250 eV) was performed to probe the VB electronic structure of Alq_3. Figure 3 compares the results of the VB-XPS measurement with the DFT calculated total DOS. After aligning the main features of the calculated DOS with those of the photoemission spectrum, it is apparent that there is an excellent agreement between photoemission and DFT up to 15 eV below E_F, with the exception of the HOMO related peak. This discrepancy between the VB-XPS and the DFT concerning the HOMO has been reported earlier.[10,11] As a result of the overall agreement between our experimental results and DFT calculation, as well as the agreement of both with those of previous studies, we are confident in our sample quality and in the accuracy of the theoretical framework used for this investigation.

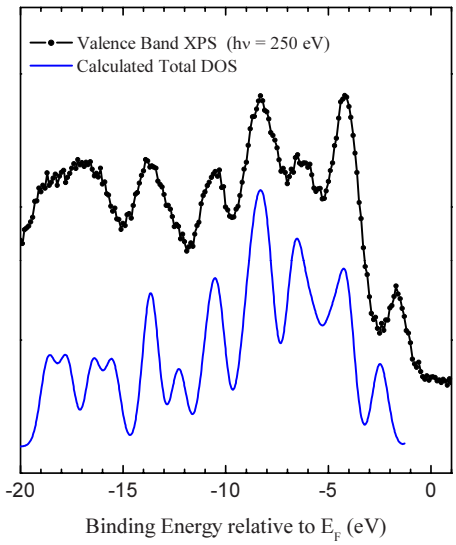

FIG. 3. (Color online) Comparison between VB-XPS and the calculated total DOS. $h\nu$=250 eV.

XPS measurement of the C 1*s* core level of Alq_3 (not shown) reveals a broad peak centered at a binding energy of 285.3 eV, which can be deconvoluted into three components. Our XPS spectra are consistent with those published earlier by Pi *et al.*,[18] and we identify the three components as corresponding to C atoms in C–C, C–H, and C–N/O environments. Consequently the C $K\alpha$ x-ray emission spectra reported here can be understood in terms of transitions from the VB into core holes on these three distinct core levels. XPS measurements of the N 1*s* and O 1*s* reveal single peaks at binding energies of 400.1 and 531.6 eV, respectively. For both N and O *K*-edges, emission and absorption transitions involve only one core level, in contrast with the C *K*-edge where the situation is more complicated.

B. X-ray photon beam induced damage

High resolution XES measurements using a Nordgren-type instrument with narrow entrance slits require a small photon spot (approximately 40 μm) with a high photon flux (10^{13} photons/s) on the sample, and long collection times (30–60 min). We have shown previously that these conditions lead to significant photon-induced beam damage in phthalocyanines,[4,7] and the same has been observed here for Alq_3. Indeed, x-ray damage to Alq_3 has been reported earlier in an XPS study, where exposure to full nonmonochroma-

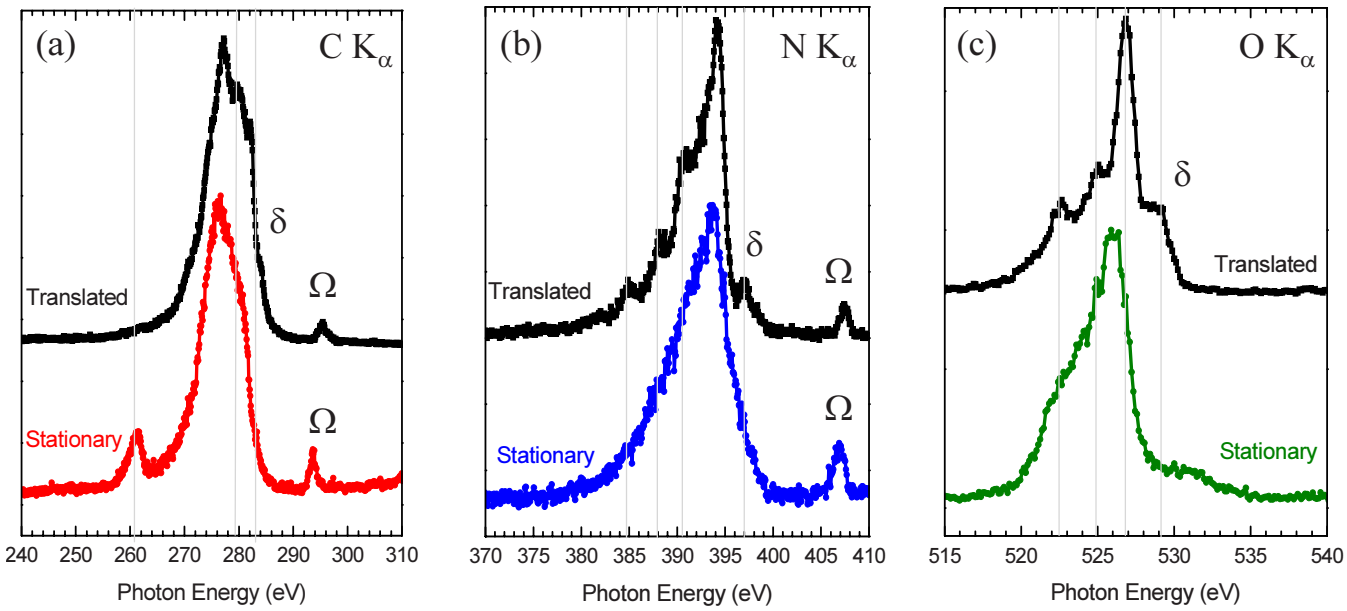

FIG. 4. (Color online) The above-threshold (a) carbon, (b) nitrogen, and (c) oxygen *K*-edge XES spectra from translated and stationary Alq_3 films. The features identified Ω and δ refer to the elastically scattered photons and emission from the HOMO state, respectively.

tized undulator radiation (10^{15} photons/s) for 5 min was found to result in dramatic changes in the N 1*s* core level, a pronounced VB broadening of all features, and irreversible damage.[11] We have solved the beam damage problem by continuously translating the Alq_3 films in front of the focused x-ray beam at 40 μm/s as spectra are being recorded. With a photon spot size of 40 μm, this translation rate ensures spectra are recorded from pristine material every second. As will be shown below, this technique has a dramatic effect on the measured XES spectra from Alq_3, similar to what we observed in Cu-Pc.[4]

Figure 4 compares the (a) carbon, (b) nitrogen, and (c) oxygen *K*-edge XES spectra for both stationary and continuously translated Alq_3 films, and illustrates clearly the effect of the x-ray photon beam. The incident excitation energies were 293.2, 407.7, and 539.0 eV, respectively. These excitation energies are well above the absorption threshold for each of the corresponding 1*s* states. The feature identified as Ω in each panel corresponds to the elastically scattered light for these excited energies. The N *K*-edge XES spectrum from the stationary film shows fewer spectral features and less definition than that from the translated film. This is expected in high defect density films since VB features will be particularly sensitive to any changes related to broken molecular bonds. In the N *K*-edge XES spectra, the pronounced peaks at approximately 384.8, 388.0, 390.5, and 397.0 eV in spectrum from the translated film are absent in the spectrum from the stationary film. The feature at 397.0 eV (marked as δ) can be identified as emission from the HOMO state. The absence of this feature in the spectra from the stationary films highlights how electronic structure information obtained from beam-damaged samples is problematic. The difference between our results from translated and stationary films is consistent with the conclusions from the XPS studies that Alq_3 partly decomposes by ejecting nitrogen out of the molecule.[11]

For the O *K*-edge XES spectra, a distinct change in the overall spectral shape is also noted between spectra recorded from stationary and translated films. The most intense peak at approximately 527 eV shifts to lower emission energy in the damaged film. This is consistent with XPS studies in which the oxygen 1*s* core level is observed to shift toward lower binding energy for damaged Alq_3.[11] A significant broadening and energy shift of the emission from the HOMO state (δ) in the XES spectrum from the damaged film can be seen in Fig. 3(c). Less dramatic changes between the emission from translated and stationary films are observed in the C *K*-edge XES spectra. This is due to the broad range of binding energies (spanning ~1.6 eV) exhibited by the C 1*s* states as a result of the different local bonding environments of the C atoms.[18] The energy spread of the C 1*s* states means that C $K\alpha$ XES spectra recorded with excitation energies far above the absorption threshold contain transitions from the VB PDOS into a wide range of C 1*s* core holes, each associated with different C atom sites. This results in the above-threshold C *K*-edge XES spectra appearing broader, and with fewer distinct spectral features, than the N and O XES *K*-edge spectra. Nevertheless, we note that the feature at ~280 eV and the HOMO state (δ) are less well defined in the spectrum from the stationary film. The emission peak at ~260 eV is due to O $K\alpha$ emission, measured in second order, observed via excitation from second order light from the monochromator, and emerges more strongly in the C *K*-edge spectrum following beam damage, potentially indicating that a change in the ratio of carbon atoms to oxygen atoms may be a component of the molecular damage. Previous XES studies of the above-threshold C and N *K*-edges by Kim *et al.*[9] share many similarities with the spectra we have recorded from stationary samples, particularly lack of distinct spectral features. We conclude that these earlier XES measurements performed on Alq_3 exhibit significant beam damage.

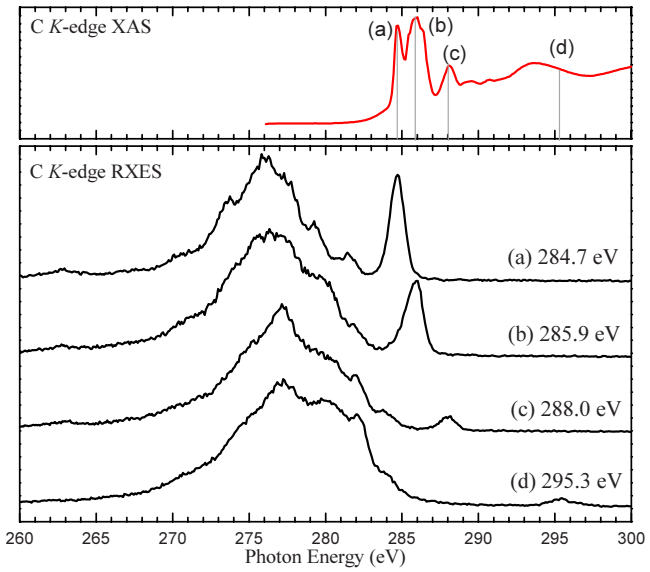

FIG. 5. (Color online) Bottom panel: RXES spectra for the C *K*-edge. Top panel: C *K*-edge XAS spectrum, with excitation energies used for the RXES spectra indicated.

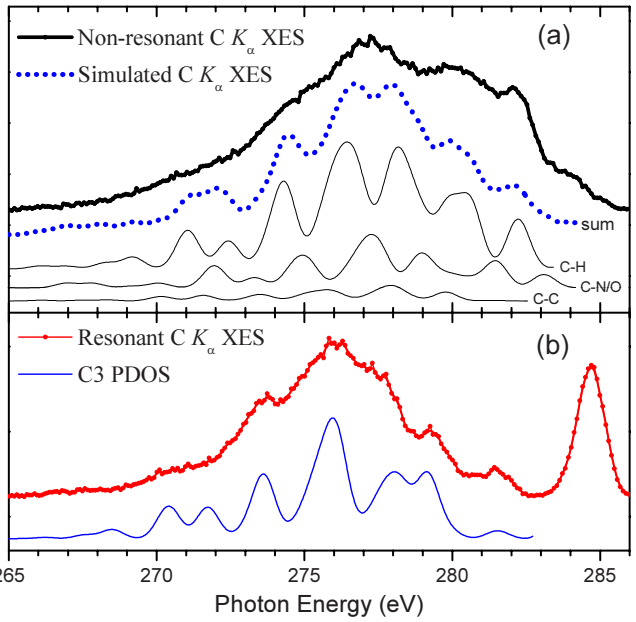

FIG. 6. (Color online) Top panel (a) comparison of nonresonant carbon *K*-edge XES spectrum with the simulated XES, as well as the 2*p* partial densities of states for carbon atoms in a C–C, C–H, and C–N/O environment, which have been shifted based on the binding energy of their core levels (see text for details). Bottom panel (b) resonant carbon *K*-edge XES spectrum due primarily by transitions on the C3 atoms, compared to the calculated PDOS for the C3 atoms. The excitation energy was 284.7 eV for the resonant spectrum and 295.3 eV for the nonresonant spectrum.

C. RXES at the carbon *K*-edge

The normalized C *K*-edge RXES spectra are displayed vertically offset to each other in the bottom panel of Fig, 5. The C *K*-edge XAS spectrum is presented in the top panel of Fig. 5 on the same calibrated photon energy axis; the photon energies used to excite the RXES spectra are identified on the XAS spectrum. We note that our XAS spectrum is in agreement with previous studies.[9,10] The LUMO lies primarily on the C1 and C3 atoms, both on the pyridyl ring, as indicated in Fig. 2(c). The first absorption feature in the XAS spectrum of Fig. 5 is primarily due to transitions to the C3 LUMO, with some contribution from transitions to the LUMO+1 state on the C4 atom. The C3 atom is in a simple C–H environment and the C3 1*s* core level lies at approximately 285.3 eV. However, since the first absorption feature is measured at 284.7 eV in Fig. 5, it appears that the LUMO has been pulled below E_F. This is likely due to the Coulomb interaction of the excited electron with the 1*s* core hole created during x-ray absorption, an effect which has been observed in studies of the electronic structure of benzene and pyridine.[19] The LUMO+1 is considerably less spatially localized and has components of comparable intensity on all but three of the ligand carbon atoms (C3, C5, and C8). The second absorption feature is fairly broad as it results from transitions not only to the LUMO+1 but also to the LUMO and LUMO+2 states.

For the XES spectrum recorded at the lowest energy of $h\nu$=284.7 eV (point "a" in the XAS spectrum), the excited electron resides in the LUMO, as indicated by the position of the elastic peak. The system does not become ionized in this case, and the excited core electron effectively screens the empty core hole state in large delocalized molecular systems, thereby reducing the effect that the core hole has on the energies of the valence states and reducing the strength of final state effects in XES spectra in comparison to photoemission measurements.[20] As the excitation energy in-creased, clear changes in the C $K\alpha$ emission spectra can be observed in Fig. 5. These changes can be explained in terms of three sets of overlapping spectra due to transitions into the three distinct C 1*s* core levels; i.e., as the excitation energy increases, electrons can be excited out of deeper core levels, making more transitions possible.

Figure 6 presents a comparison between the measured resonant and nonresonant C *K*-edge and the results of a DFT calculation of the C 2*p* VB PDOS. When making such comparisons, it is important to take into account the different core levels associated with distinct chemical sites for the same element. In order to compare the C $K\alpha$ XES spectra to our DFT calculated C 2*p* PDOS, we first broadened the PDOS by convoluting it with a Voigt function that appropriately accounts for core hole lifetime effects ($\omega_L \sim 0.3$ eV) and for the spectrometer energy resolution ($\omega_G \sim 0.4$ eV). Transitions into core holes with greater binding energy result in higher energies for the emitted photons, and so features of the calculated PDOS associated with carbon in a C–H environment (C2, C3, C5, C6, and C7 in Fig. 1) were shifted upward by +0.85 eV, while features associated with a C–N or C–O environment (C1, C8, and C9) were shifted by +1.7 eV, in accordance with C 1*s* XPS results of Pi *et al.*[18] The resulting "simulated x-ray emission spectrum" was then rigidly shifted in order to align the most intense peaks with those of the measured XES spectra. Figure 6(a) presents the comparison between the above-threshold, nonresonant XES, and the calculated PDOS. Good agreement is found in terms of both the energetic locations of the peaks and the overall spectral shape. Figure 6(b) presents the emission spectrum for the lowest resonant energy [spectrum (a) in Fig. 5], and com-

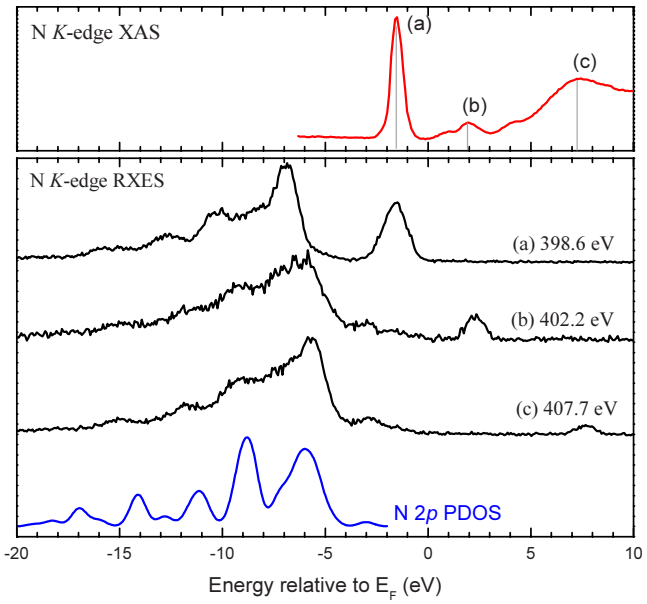

FIG. 7. (Color online) Bottom panel: RXES spectra for the N *K*-edge. Top panel: N *K*-edge XAS spectrum, with excitation energies used for the RXES spectra indicated. The calculated nitrogen 2*p* PDOS is included in the bottom panel.

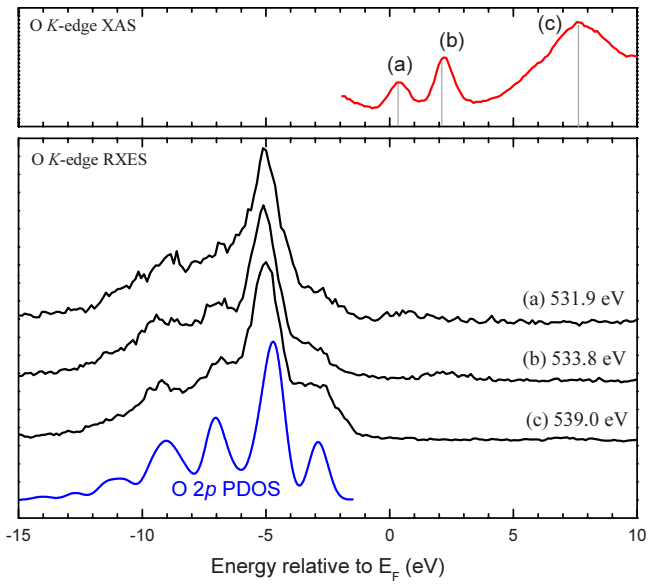

FIG. 8. (Color online) Bottom panel: RXES spectra for the O *K*-edge. Top panel: O *K*-edge XAS spectrum, with excitation energies used for the RXES spectra indicated. The calculated oxygen 2*p* PDOS is included in the bottom panel.

pares it to the calculated PDOS associated only with the C3 atoms. As noted above, the first absorption peak is primarily due to transitions to the LUMO on the C3 atom. As a result, the first resonant XES spectrum should be an accurate measurement of the VB PDOS associated with the C3 atoms. Excellent agreement is found between experiment and theory as seen in Fig. 6(b). Any differences can reasonably be attributed to the fact that the first resonant peak has minor contributions from the C2 and C4 atoms. However, in order to line up properly with the first resonant peak, the energy scale for the C3 PDOS has been shifted downward by 0.7 eV relative to the PDOS shown in Fig. 6(a), indicating that the resonant spectrum is at a lower emission energy than one would expect. This is likely due to screening from the LUMO-excited electron, which is not present in the nonresonant case.[20]

D. RXES at the nitrogen and oxygen *K*-edges

The normalized N *K*-edge RXES spectra are displayed vertically offset to each other in the bottom panel of Fig. 7, together with the calculated 2*p* VB PDOS. The N *K*-edge XAS spectrum is presented in the top panel of Fig. 7 on the same calibrated photon energy axis; the photon energies used to excite the RXES spectra are identified on the XAS spectrum. The N *K*-edge XAS is in agreement with earlier XAS studies by Curioni *et al.*[10] A common energy scale for nitrogen emission and absorption spectra is used and referenced to E_F, corresponding to a photon energy of 400.1 eV. The intense first peak in the XAS spectrum is associated with transitions from the N 1*s* state to the LUMO, and lies below the Fermi energy for reasons discussed previously for the C *K*-edge.[11,19] The weaker second and third peaks are associated with transitions from the N 1*s* core level to the LUMO+2 and LUMO+3 states, respectively. The corresponding RXES spectra for the N 1*s* to LUMO and LUMO +3 incident energies are plotted along with the above-threshold XES spectrum on the same calibrated photon energy axis in the bottom panel of Fig. 7. Elastic peaks are again observed for the corresponding energies. The HOMO state is easily discernable and we have rigidly shifted the calculated N 2*p* PDOS so that energies of the observed and calculated HOMO match. No core level shifts are required for the calculated PDOS because there is only one nitrogen site, and hence only one binding energy for the N 1*s* state in the molecule. The above-threshold XES spectrum reflects the N 2*p* PDOS, and we observe agreement between the energetic positions of the XES and occupied PDOS peaks. It is apparent from Fig. 7 that the first resonant N *K*-edge emission spectrum (a), while showing the same overall structure as the nonresonant case, is shifted toward lower emission energy by approximately 1.4 eV. This is not due to any chemical shift, since there is only one nitrogen environment. This shift must be due to screening from the LUMO-excited electron, as we have already seen for carbon.[20] This, along with the presence of the first XAS peak below the Fermi level, indicates that for Alq_3, nitrogen in its 1*s* LUMO-excited state behaves much in the same way as carbon, with respect to electron screening effects.

The normalized O *K*-edge RXES spectra are displayed vertically offset to each other in the bottom panel of Fig. 8, together with the calculated O 2*p* VB PDOS. The O *K*-edge XAS spectrum is presented in the top panel of Fig. 8 on the same calibrated photon energy axis; the photon energies used to excite the RXES spectra are identified on the XAS spectrum. E_F corresponds to an emission/absorption energy of 531.6 eV. There is little O contribution to the unoccupied states in Alq_3, and this is reflected by the lower relative intensity of the absorption spectrum for the O *K*-edge. It should be noted that neither the O *K*-edge XAS nor the

RXES [Fig. 8(a)] shows signs of screening effects from the LUMO-excited electron, in contrast with the carbon and nitrogen *K*-edges. The above-threshold XES spectrum (c) agrees well with the calculated O $2p$ PDOS in terms of both the spectral shape and the relative intensity of the peaks, and emission from the oxygen HOMO is easily discernable.

V. CONCLUSION

The element-specific electronic structure of the organic semiconductor Alq_3 has been studied using a combination of XES, XPS, and XAS, and compared to the results of DFT calculations. Severe photon-induced beam damage was observed, but could be circumvented by continuously translating large area films in front of the photon beam as spectra were recorded. The calculated nitrogen and oxygen $2p$ PDOSs were found to agree well with the corresponding *K*-edge resonant and nonresonant emission spectra. In the case of carbon, we have shown that by appropriately adjusting the calculated PDOS for chemical shifts, it is possible to produce an accurate reflection of measured emission spectra.

ACKNOWLEDGMENTS

This work was supported in part by the NSF under Grant No. CHE-0807368, and by the U.S. Air Force Office of Scientific Research under Grant No. FA9550-06-1-0157. The spectrometer system was funded by the U.S. Army Research Office under Grant Nos. DAAD19-01-1-0364 and DAAH04-95-0014. The Trinity College Dublin group acknowledges the financial support of Science Foundation Ireland. The NSLS was supported by the U.S. Department of Energy, Office of Science, Office of Basic Energy Sciences, under Contract No. DE-AC02-98CH10886.

[1] S. R. Forrest, Chem. Rev. (Washington, D.C.) **97**, 1793 (1997); S. R. Forrest, IEEE J. Quantum Electron. **6**, 1072 (2000).
[2] A. Kimyonok, X. Y. Wang, and M. Weck, Polym. Rev. **46**, 47 (2006).
[3] A. Kotani and S. Shin, Rev. Mod. Phys. **73**, 203 (2001).
[4] J. E. Downes, C. McGuinness, P.-A. Glans, T. Learmonth, D. Fu, P. Sheridan, and K. E. Smith, Chem. Phys. Lett. **390**, 203 (2004).
[5] N. Peltekis, B. Holland, L. F. J. Piper, A. DeMasi, K. E. Smith, J. E. Downes, I. T. McGovern, and C. McGuinness, Appl. Surf. Sci. **255**, 764 (2008).
[6] Y. Zhang, T. Learmonth, S. Wang, A. Y. Matsuura, J. Downes, L. Plucinski, S. Bernardis, C. O'Donnell, and K. E. Smith, J. Mater. Chem. **17**, 1276 (2007).
[7] Y. Zhang, S. Wang, T. Learmonth, L. Plucinski, A. Y. Matsuura, S. Bernardis, C. O'Donnell, J. E. Downes, and K. E. Smith, Chem. Phys. Lett. **413**, 95 (2005).
[8] Y. Zhang, S. Wang, A. Demasi, I. Reid, L. F. J. Piper, A. Y. Matsuura, J. E. Downes, and K. E. Smith, J. Mater. Chem. **18**, 1792 (2008).
[9] P. S. G. Kim, S. J. Naftel, T. K. Sham, I. Coulthard, Y. F. Hu, A. Moewes, and J. W. Freeland, J. Electron Spectrosc. Relat. Phenom. **144–147**, 901 (2005).
[10] A. Curioni, W. Andreoni, R. Treusch, F. J. Himpsel, E. Haskal, P. Seidler, C. Heske, S. Kakar, T. van Buuren, and L. J. Terminello, Appl. Phys. Lett. **72**, 1575 (1998).
[11] R. Treusch, F. J. Himpsel, S. Kakar, L. J. Terminello, C. Heske, T. van Buuren, V. V. Dinh, H. W. Lee, K. Pakbaz, G. Fox, and I. Jimenez, J. Appl. Phys. **86**, 88 (1999).
[12] J. Nordgren and N. Wassdahl, Phys. Scr., T **31**, 103 (1989).
[13] J. Nordgren and N. Wassdahl, J. Electron Spectrosc. Relat. Phenom. **72**, 273 (1995).
[14] J. Nordgren, G. Bray, S. Cramm, R. Nyholm, J. E. Rubensson, and N. Wassdahl, Rev. Sci. Instrum. **60**, 1690 (1989).
[15] *X-Ray Data Booklet*, edited by A. C. Thompson *et al.* (Lawrence Berkeley National Laboratory, University of California, Berkeley, CA, 2001); http://xdb.lbl.gov/.
[16] X. Chen, P. A. Glans, X. Qiu, S. Dayal, W. D. Jennings, K. E. Smith, C. Burda, and J. Guo, J. Electron Spectrosc. Relat. Phenom. **162**, 67 (2008).
[17] J. P. Zhang and G. Frenking, J. Phys. Chem. A **108**, 10296 (2004).
[18] T. W. Pi, T. C. Yu, C. P. Ouyang, J. F. Wen, and H. L. Hsu, Phys. Rev. B **71**, 205310 (2005).
[19] J. A. Horsley, J. Stohr, A. P. Hitchcock, D. C. Newbury, A. L. Johnson, and F. Sette, J. Chem. Phys. **83**, 6099 (1985).
[20] H. Ågren, Y. Luo, F. Gelmukhanov, H. Jørgen, and A. Jensen, J. Electron Spectrosc. Relat. Phenom. **82**, 125 (1996).